Design of a Linear-Quadratic Regulator for the Control of an Oil-Heating Tank. Modeling and Simulation

José M. Campos-Salazar
jcampossalazar@gmail.com

***Abstract*— In this paper, an oil-heating tank is presented, developing its respective modeling through the application of the laws of conservation of mass and energy. Then a set of nonlinear differential equations are obtained representative of the process. Subsequently, this model is linearized obtaining its linearized model. With this linear model, the design of two control systems is presented, based on a PI feedback output compensator and based on a linear-quadratic regulator, where the control objectives are the storage temperature and the fuel oil level. Finally, the process is simulated, verifying the feasibility of the operation with the designed control system.**

Keywords*—LQR, m*ass- and energy-balance, PI-compensator, non-linear equations, oil-heating tank, simulation.

I. INTRODUCTION

In most of the industries that handle fuel oil, it is required to store this product in tanks for later use. Precisely the storage condition, can generate that the physical properties of the fuel oil can change undesirably, as its viscosity, for example, due to the temperature gradients that could be affected. Therefore, a temperature regulation system is required and necessary to maintain its properties undisturbed.

An oil-heating tank is the simple and safe solution for maintaining the temperature and thus preserving the viscosity of the fuel oil. Therefore, in addition to having the necessary tank for storage, it is also required to have a thermal system to supply energy to the fuel oil. It is therefore required to have a temperature control system. In addition, as the tank has overflow safety levels, a level control is also a must.

It is interesting to note that there are not many works that address these two control goals, in fact, in most of them, they cover the temperature control as the main one, leaving in second place, the level of the tank, assuming steady state conditions regarding the level [1]–[5].

In this paper, an oil-heating tank is presented, developing its respective modeling through the application of the laws of conservation of mass and energy. Then a set of nonlinear differential equations are obtained representative of the process. Subsequently, this model is linearized obtaining its linearized model. With this linear model, the design of two control systems is presented, based on a PI feedback output compensator and based on a linear-quadratic regulator, where the control targets are the storage temperature and the fuel oil level. Finally, the process is simulated, verifying the feasibility of the operation with the designed control system.

II. PROCESS DESCRIPTION

The process and instrumentation diagram of the proposed oil-heating tank is presented in Fig. 1. From Fig. 1 it can be seen that the system is configured with a tank named TK-100 which is working as a heat exchanger. It has three inlet pipes and one outlet pipe. The first inlet is the volumetric flow of the oil to be processed, which flows from an external process unit. This inlet is associated with the following dynamic variables $f_1(t)$, $T_1(t)$, and $P_1(t)$, which are the flow, the temperature, and the pressure, respectively. In addition, the piping of this inlet is connected to the tank at a height of H_d measured form the ground. The second inlet is the saturated steam flow, supplied by a generator unit external to this process, which allows to supply heat to the oil, through its flow, by a heating coil located inside the tank. The heating coil is built by a metal tube of thickness 20 BWG. The dynamic variables of the steam are the mass flow $w_s(t)$, the temperature $T_s(t)$, and its saturation pressure $P_s(t)$. The third input is the constant volumetric flow of inert gas f_N which allows maintaining a constant pressure (P_2) inside the tank above the oil level, due to the presence of a blanket of this inert gas. Finally, the output of the TK-100 is the oil already processed and reaching the reference temperature ($T^*_3(t)$). The dynamic variables of the outlet are the flow $f_3(t)$, its temperature $T_3(t)$, and its pressure $P_3(t)$.

The process assumptions are that the TK-100 is well insulated, the physical properties of the oil are not relatively strong temperature-dependent functions [6], [7], the liquid (oil) inside the tank is well mixed, the liquid level completely covers the heating coil, constant and uniform densities, specific heats, and steam latent heat. Moreover, the metal of

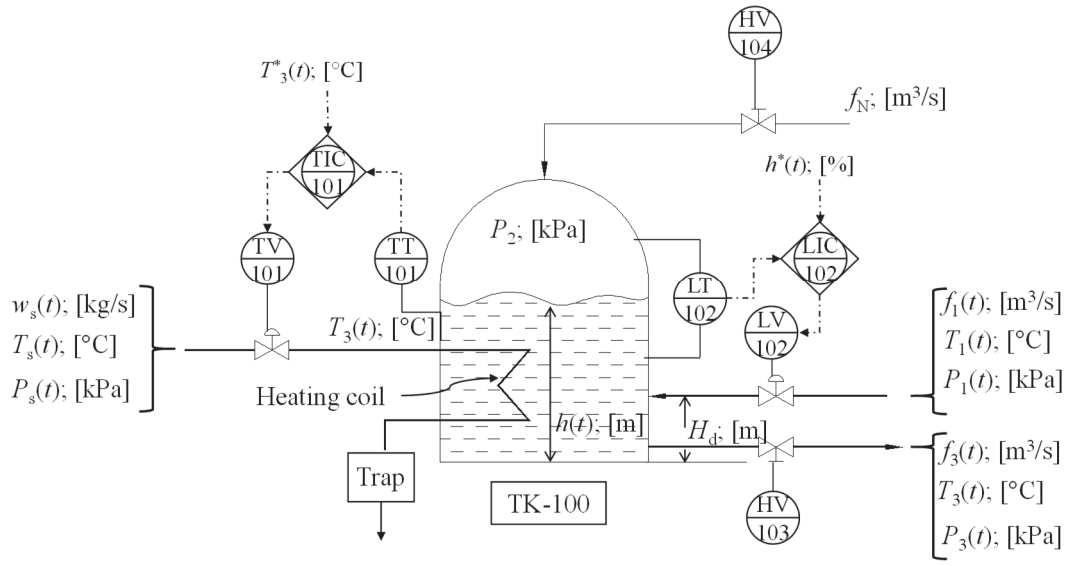

Fig. 1. Oil-heating tank process.

the tank and heating coil is at the same temperature as the condensing steam, negligible heat losses and transportation lags, and finally, constant pressure drop across the steam valve. Condensation from the heating coil is trapped by a vapor trap (trap) and conducted to another process unit, also external.

From the above assumptions, it can be concluded that the temperature of the oil inside the tank is the same as that of the outlet, i.e. $T_3(t)$. The height of the level related to the liquid inside the TK-100 is labeled as $h(t)$.

The volumetric flows, mass flow, temperatures, height, and pressures are measured in m^3/s, kg/s, °C, m, and kPa respectively.

From Fig. 1 it can be inferred that the control philosophy corresponds to controlling $T_3(t)$ and $h(t)$, which are the controlled variables of the system, through the manipulation of valves TV-101 and LV-102 respectively. The temperature $T_3(t)$ and the height $h(t)$ are measured through the transmitters TT-101 and LT-102 respectively. Finally, the controllers associated to the controlled variables are TIC-101 and LIC-102 respectively. On the other hand, there are two uncontrolled valves whose position is fixed. These valves are HV-104 and HV-103 and throttle the flows f_N and $f_3(t)$ respectively.

III. Process Modeling

The mass and energy balances [6]–[8] developed for the process shown in Fig. 1 are presented below. From the synthesis of these balances, the nonlinear model of the system is obtained and shown.

A. Mass and Energy Balance

Through the use of the law of conservation of mass, the differential equation that relates the height $h(t)$ is obtained and presented in (1).

$$\frac{dh(t)}{dt} = \frac{1}{A_{TK-100}} \cdot \big(f_1(t) - f_3(t)\big), \tag{1}$$

where ATK-100 is the cross-sectional areas of the TK-100 in m^2. This area is uniform throughout.

On the other hand, the energy balances around the TK-100, which is related to $T_3(t)$ and the heating coil, which is also related to $T_s(t)$ are presented in (2) and (3) respectively. It should be noted that for deriving the energy balance related to the TK-100, it is assumed that the volume of the liquid in the tank is fairly constant, for a given operating height, i.e., the level control LIC-102 operates properly.

$$\begin{aligned} \frac{dT_3(t)}{dt} = \\ = \frac{1}{c_v \cdot \rho \cdot V_{TK-100}} \cdot \big(c_p \cdot \rho \cdot f_1(t) \cdot T_1(t) + \\ + U \cdot A_h \cdot \big(T_s(t) - T_3(t)\big) - \\ - c_p \cdot \rho \cdot f_3(t) \cdot T_3(t)\big) \end{aligned} \tag{2}$$

$$\begin{aligned} \frac{dT_s(t)}{dt} = \frac{1}{C_M} \cdot (\lambda_s \cdot w_s(t) - \\ - U \cdot A_h \cdot \big(T_s(t) - T_3(t)\big)\big), \end{aligned} \tag{3}$$

where ρ, c_v, and c_p are the density and heat capacities at constant volume and pressure of the oil, measured in kg/m^3 and in kJ/kg-°C respectively. In addition, U, V_{TK-100}, A_h, C_M, and λ_s are the total heat transfer coefficient, the effective volume ($= A_{TK}.100 \cdot h$) of the tank, the cross section and heat capacity of the

$$\begin{cases} \frac{\mathrm{d}h(t)}{\mathrm{d}t} = \frac{1}{A_{\mathrm{TK-100}}} \cdot \left(c_{\mathrm{LV-102}} \cdot vp_{\mathrm{LV-102}}(t) \cdot \sqrt{\frac{P_1(t) - P_2 - \rho \cdot g \cdot (h(t) - H_{\mathrm{d}})}{G_{\mathrm{f}}}} - \right. \\ \left. - c_{\mathrm{HV-103}} \cdot \sqrt{\frac{P_1(t) + \rho \cdot g \cdot h(t) - P_3(t)}{G_{\mathrm{f}}}} \right) \\ \frac{\mathrm{d}T_3(t)}{\mathrm{d}t} = \frac{1}{c_{\mathrm{v}} \cdot \rho \cdot V_{\mathrm{TK-100}}} \cdot \left(c_{\mathrm{p}} \cdot \rho \cdot c_{\mathrm{LV-102}} \cdot T_1(t) \cdot vp_{\mathrm{LV-102}}(t) \cdot \sqrt{\frac{P_1(t) - P_2 - \rho \cdot g \cdot (h(t) - H_{\mathrm{d}})}{G_{\mathrm{f}}}} + \right. \\ \left. + U \cdot A_{\mathrm{h}} \cdot \left(T_{\mathrm{s}}(t) - T_3(t) \right) - c_{\mathrm{p}} \cdot \rho \cdot c_{\mathrm{HV-103}} \cdot T_3(t) \cdot \sqrt{\frac{P_1(t) + \rho \cdot g \cdot h(t) - P_3(t)}{G_{\mathrm{f}}}} \right) \\ \frac{\mathrm{d}T_{\mathrm{S}}(t)}{\mathrm{d}t} = \frac{1}{C_{\mathrm{M}}} \cdot \left(\lambda_{\mathrm{s}} \cdot c_{\mathrm{TV-101}} \cdot vp_{\mathrm{TV-101}}(t) - U \cdot A_{\mathrm{h}} \cdot \left(T_{\mathrm{s}}(t) - T_3(t) \right) \right). \end{cases} \tag{7}$$

heating coil, and the latent heat of condensation respectively. Each of these process constants are measured in W/m^2-°C, in m^3, in m^2, in kJ/°C, and in kJ/kg respectively.

From Fig. 1 and according to [1] the expressions of the flows $w_s(t)$, $f_1(t)$, and $f_3(t)$ are a function of the pressure drops, through the valves TV-101, LV-102, and HV-103 respectively and are presented in equations (4)–(6) (it is not necessary to consider the dynamics of the flow f_N, since this flow does not play a role in the balances in (1)–(3).

$$w_{\mathrm{s}}(t) = c_{\mathrm{TV-101}} \cdot vp_{\mathrm{TV-101}}(t) \tag{4}$$

$$f_1(t) = c_{\mathrm{LV-102}} \cdot vp_{\mathrm{LV-102}}(t) \cdot \cdot \sqrt{\frac{P_1(t) - P_2 - \rho \cdot g \cdot (h(t) - H_{\mathrm{d}})}{G_{\mathrm{f}}}} \tag{5}$$

$$f_3(t) = c_{\mathrm{HV-103}} \cdot \sqrt{\frac{P_1(t) + \rho \cdot g \cdot h(t) - P_3(t)}{G_{\mathrm{f}}}}. \tag{6}$$

Here g and G_f are the gravitational acceleration and specific density of the oil measured in m/s^2 and dimensionless, respectively. Moreover, $c_{\mathrm{TV-101}}$, $c_{\mathrm{LV-102}}$, and $c_{\mathrm{HV-103}}$ are the valve coefficients of the TV-101, LV-102, and HV-103, respectively.

Replacing (4)–(6) in (1)–(3) the non-linear model of the oil-heating tank is obtained and presented in (7).

From (7) it should be noted that $C_M = \rho_m \cdot L_m \cdot c_{pm}$ where ρ_m, L_m, and c_{pm} are the mass, linear length, and heat transfer coefficient of the metal tube of the heating coil [6]. The units of these constants are kg/m, m, and kJ/kg-°C respectively.

In the following section the linear model of the system will be obtained and presented.

B. State-Space Model of the Process

In order to design a linear controller, such as a proportional-integral (PI) compensator or a linear-quadratic regulator (LQR) [9]–[11], it is required to linearize the model of (7), thus obtaining the state-space model. The linearization obtained is based on the steady-state operating points [12], [13] that are the outcome of developing the system of equations shown in (8) and that is achieved by forcing the derivatives to zero, i.e., $\mathrm{d}h(t)/\mathrm{d}t = \mathrm{d}T_3(t)/\mathrm{d}t = \mathrm{d}T_s(t)/\mathrm{d}t = 0$. Then, replacing the time variables by their steady-state variables. Note that the steady-state variables are presented by capital letters and a superscript ss.

The unknowns of the system of equations in (8) are the positions of the valves LV-102 and TV-101, i.e., $VP^{ss}_{\mathrm{LV-102}}$ and $VP^{ss}_{\mathrm{TV-101}}$ respectively, and the saturated steam temperature, i.e., T^{ss}_s. The other variables are all known and given. Table I lists all the constants and steady state variables of the process. The solution of (8) are presented in equations (9)–(11).

Having the steady state operating points it is possible to linearize the model in (7) [12]. Applying the Taylor series expansion to (7) around the operating points in (9)–(11), the linear model, as a function of deviation variables, of the process is obtained and shown in (12). In this case, where all auxiliary constants present in (12) are defined in (13)–(15).

The deviation variables are $\hat{h}(t) = h(t) - H^{ss}$, $\hat{T}_3(t) = T_3(t) - T_3{}^{ss}$, $\hat{T}_s(t) = T_s(t) - T_s^{ss}$, $\widehat{vp}_{\mathrm{LV-102}}(t) = vp_{\mathrm{LV-102}}(t) - VP^{ss}_{\mathrm{LV-102}}$, $\hat{P}_1(t) = P_1(t) - P_1^{ss}$, $\hat{P}_3(t) = P_3^{ss}$, $\hat{T}_1(t) = T_1(t) - T_1^{ss}$, $\widehat{vp}_{\mathrm{TV-101}}(t) = vp_{\mathrm{TV-101}}(t) - VP^{ss}_{\mathrm{TV-101}}$. Finally, from the linear model of the process described in (12), the state-space model is obtained and described in (16).

The vectors and matrices are defined in (17) and (18) respectively [12]–[14]. Here $\{\hat{\mathbf{x}}, \hat{\mathbf{y}}\} \in \{\mathbb{R}^3\}$ and $\hat{\mathbf{u}} \in \{\mathbb{R}^5\}$, $\{\mathbf{A_m}, \mathbf{C_m}\} \in \mathcal{M}_{3x3}\ \{\mathbb{R}\}$, and $\{\mathbf{B_m}, \mathbf{D_m}\} \in \mathcal{M}_{3x5}\ \{\mathbb{R}\}$.

IV. Control System Design

The following section presents the designs of two linear controllers, which are applied to the oil-heating tank. The first controller is based on a PI compensator and the second one is based on an LQR.

$$\begin{cases} c_{\mathrm{LV-102}} \cdot VP^{\mathrm{ss}}_{\mathrm{LV-102}} \cdot \sqrt{\frac{P^{\mathrm{ss}}_1 - P^{\mathrm{ss}}_2 - \rho \cdot g \cdot (H^{\mathrm{ss}} - H_{\mathrm{d}})}{G_{\mathrm{f}}}} - c_{\mathrm{HV-103}} \cdot \sqrt{\frac{P^{\mathrm{ss}}_1 + \rho \cdot g \cdot H^{\mathrm{ss}} - P^{\mathrm{ss}}_3}{G_{\mathrm{f}}}} = 0 \\ c_{\mathrm{p}} \cdot \rho \cdot c_{\mathrm{LV-102}} \cdot T^{\mathrm{ss}}_1 \cdot VP^{\mathrm{ss}}_{\mathrm{LV-102}} \cdot \sqrt{\frac{P^{\mathrm{ss}}_1 - P^{\mathrm{ss}}_2 - \rho \cdot g \cdot (H^{\mathrm{ss}} - H_{\mathrm{d}})}{G_{\mathrm{f}}}} + \\ + U \cdot A_{\mathrm{h}} \cdot (T^{\mathrm{ss}}_{\mathrm{s}} - T^{\mathrm{ss}}_3) - c_{\mathrm{p}} \cdot \rho \cdot c_{\mathrm{HV-103}} \cdot T^{\mathrm{ss}}_3 \cdot \sqrt{\frac{P^{\mathrm{ss}}_1 + \rho \cdot g \cdot H^{\mathrm{ss}} - P^{\mathrm{ss}}_3}{G_{\mathrm{f}}}} = 0 \\ \lambda_{\mathrm{s}} \cdot c_{\mathrm{TV-101}} \cdot VP^{\mathrm{ss}}_{\mathrm{TV-101}} - U \cdot A_{\mathrm{h}} \cdot (T^{\mathrm{ss}}_{\mathrm{s}} - T^{\mathrm{ss}}_3) = 0. \end{cases} \tag{8}$$

$$VP^{\mathrm{ss}}_{\mathrm{LV-102}} = \frac{c_{\mathrm{HV-103}} \cdot \sqrt{\frac{P^{\mathrm{ss}}_2 - P^{\mathrm{ss}}_3 + \rho \cdot g \cdot H^{\mathrm{ss}}}{G_{\mathrm{f}}}}}{c_{\mathrm{LV-102}} \cdot \sqrt{\frac{P^{\mathrm{ss}}_1 - P^{\mathrm{ss}}_2 + \rho \cdot g \cdot (H_{\mathrm{d}} - H^{\mathrm{ss}})}{G_{\mathrm{f}}}}} \tag{9}$$

$$VP^{\mathrm{ss}}_{\mathrm{TV-101}} = \frac{c_{\mathrm{p}} \cdot c_{\mathrm{HV-103}} \cdot \rho \cdot \sqrt{\frac{P^{\mathrm{ss}}_2 - P^{\mathrm{ss}}_3 + \rho \cdot g \cdot H^{\mathrm{ss}}}{G_{\mathrm{f}}}}}{c_{\mathrm{TV-101}} \cdot \lambda_{\mathrm{s}}} (T^{\mathrm{ss}}_3 - T^{\mathrm{ss}}_1) \tag{10}$$

$$T^{\mathrm{ss}}_{\mathrm{s}} = T^{\mathrm{ss}}_3 + \frac{c_{\mathrm{p}} \cdot c_{\mathrm{HV-103}} \cdot \rho \cdot \sqrt{\frac{P^{\mathrm{ss}}_2 - P^{\mathrm{ss}}_3 + \rho \cdot g \cdot H^{\mathrm{ss}}}{G_{\mathrm{f}}}}}{A_{\mathrm{h}} \cdot U} \cdot (T^{\mathrm{ss}}_3 - T^{\mathrm{ss}}_1). \tag{11}$$

$$\begin{cases} \frac{\mathrm{d}\hat{h}(t)}{\mathrm{d}t} = K_{11} \cdot \hat{h}(t) + K_{12} \cdot \widehat{vp}_{\mathrm{LV-102}}(t) + K_{13} \cdot \hat{P}_1(t) + K_{14} \cdot \hat{P}_3(t) \\ \frac{\mathrm{d}\hat{T}_3(t)}{\mathrm{d}t} = K_{21} \cdot \hat{T}_3(t) - K_{21} \cdot \hat{T}_{\mathrm{s}}(t) + K_{22} \cdot \widehat{vp}_{\mathrm{LV-102}}(t) + K_{23} \cdot \hat{T}_1(t) + K_{24} \cdot \hat{P}_1(t) + K_{25} \cdot \hat{P}_3(t) + K_{26} \cdot \hat{h}(t) \\ \frac{\mathrm{d}\hat{T}_{\mathrm{s}}(t)}{\mathrm{d}t} = K_{31} \cdot \hat{T}_{\mathrm{s}}(t) - K_{31} \cdot \hat{T}_3(t) + K_{32} \cdot \widehat{vp}_{\mathrm{TV-101}}(t), \end{cases} \tag{12}$$

TABLE I. CONSTANTS AND STEADY STATE VARIABLES OF THE PROCESS

Variables	Values
ρ	848.979 kg/m^3
c_{p}	1.8841 kJ/kg-°C
c_{v}	1.8841 kJ/kg-°C
G_{f}	$\rho/1000 \approx 0.8490$
g	9.81 m/s^2
A_{h}	11.845 m^2
L_{m}	296.875 m
ρ_{m}	0.265 kg/m^3
c_{pm}	0.502 kJ/kg-°C
U	771 W/m^2-°C
C_{M}	39.4933 kJ/°C
λ_{s}	2,030.6 kJ/kg
D (tank diameter)	3 m
$A_{\mathrm{TK-100}}$	$0.25 \cdot \pi \cdot D^2 \approx 7.0686$ m^2
$h_{\max}$ (Maximum tank height)	2.5 m
$V_{\mathrm{TK-100}}$	7.0686 m^3
H_{d}	1.5 m
H^{ss}	$0.5 \cdot h_{\max} \approx 1.25$ m
$F^{\mathrm{ss}}{}_1$	10 m^3/s
$T^{\mathrm{ss}}{}_1$	21.11 °C
$T^{\mathrm{ss}}{}_3$	93.33 °C
$T^{\mathrm{ss}}{}_{\mathrm{s}}$	175 °C
$P^{\mathrm{ss}}{}_{\mathrm{s}}$	792.897 kPa
$P^{\mathrm{ss}}{}_1$	31.026 kPa
$P^{\mathrm{ss}}{}_2$	276 kPa
$P^{\mathrm{ss}}{}_3$	103.421 kPa
$VP^{\mathrm{ss}}{}_{\mathrm{LV-102}}$	0.31 per unit
$VP^{\mathrm{ss}}{}_{\mathrm{TV-101}}$	0.041 per unit
$c_{\mathrm{LV-102}}$	$8.57 \cdot 10^{-3}$
$c_{\mathrm{HV-103}}$	$8 \cdot 10^{-5}$
$c_{\mathrm{TV-101}}$	1.174

The data of the transmitter are the gains and time constants of each transmitter, i.e., $K_{\mathrm{TT-101}}$, $K_{\mathrm{LT-102}}$, $\tau_{\mathrm{TT-101}}$, and $\tau_{\mathrm{LT-102}}$ respectively are listed in Table II. In addition, the dynamics of the transmitters are modeled as first order responses [1]. Although the TT-101 does not perform any conversion in the measurement, i.e., it reads degrees °C, the LT-102 converts the measurement from m to %, since, in normal, tank capacities are measured as a percentage of their maximum height, i.e., hmax. The scale of TT-101 and LT-102 are [0, 3.048] m and [0, 149] °C respectively.

A. PI-Compensator Design

By applying the Laplace transform to the linear model (12), considering zero initial conditions, the open-loop model of the oil-heating tank is shown in (19). In addition, the block diagram of the linearized process is depicted in Fig. 2.

From (19), s is the Laplace operator. From Fig. 2 it is possible to identify the two transfer functions related to the control loops TIC-101 and LIC-102. Regarding TIC-101 the transfer function relating $\hat{T}_3(s)$ and $\widehat{VP}_{\mathrm{TV-101}}(s)$ is presented in (20). Related to LIC-102 the transfer function relating $\hat{H}(s)$ and $\widehat{VP}_{\mathrm{LV-102}}(s)$ is shown in (21).

$$\frac{\hat{H}(s)}{\widehat{VP}_{\mathrm{LV-102}}(s)} = \frac{K_{12}}{s - K_{11}} \tag{20}$$

$$\frac{\hat{T}_3(s)}{\widehat{VP}_{\mathrm{TV-101}}(s)} = \frac{K_{21} \cdot K_{31}}{(s - K_{21}) \cdot (s - K_{31})}. \tag{21}$$

In order to design the PI compensators for TIC-101 and LIC 102, the transient analysis (step response) and root locus diagrams of (20) and (21) are obtained and shown in Fig. 3(a) and (b), and Fig.

$$\begin{cases} K_{11} = -\frac{1}{2}\cdot\frac{\rho\cdot g}{A_{\mathrm{TK-100}}}\cdot\left(c_{\mathrm{LV-102}}\cdot VP^{\mathrm{SS}}_{\mathrm{LV-102}}\cdot\sqrt{\frac{G_{\mathrm{f}}}{P^{\mathrm{SS}}_1-P^{\mathrm{SS}}_2-\rho\cdot g\cdot(H^{\mathrm{SS}}-H_{\mathrm{d}})}}+\right. \\ \left.+c_{\mathrm{HV-103}}\cdot\sqrt{\frac{G_{\mathrm{f}}}{P^{\mathrm{SS}}_1+\rho\cdot g\cdot H^{\mathrm{SS}}-P^{\mathrm{SS}}_3}}\right) \\ K_{12} = \frac{c_{\mathrm{LV-102}}}{A_{\mathrm{TK-100}}}\cdot\sqrt{\frac{P^{\mathrm{SS}}_1-P^{\mathrm{SS}}_2-\rho\cdot g\cdot(H^{\mathrm{SS}}-H_{\mathrm{d}})}{G_{\mathrm{f}}}} \\ K_{13} = \frac{1}{2}\cdot\left(\frac{c_{\mathrm{LV-102}}\cdot VP^{\mathrm{SS}}_{\mathrm{LV-102}}}{A_{\mathrm{TK-100}}}\cdot\sqrt{\frac{G_{\mathrm{f}}}{P^{\mathrm{SS}}_1-P^{\mathrm{SS}}_2-\rho\cdot g\cdot(H^{\mathrm{SS}}-H_{\mathrm{d}})}}-\right. \\ \left.-\frac{c_{\mathrm{HV-103}}}{A_{\mathrm{TK-100}}}\cdot\sqrt{\frac{G_{\mathrm{f}}}{P^{\mathrm{SS}}_1+\rho\cdot g\cdot H^{\mathrm{SS}}-P^{\mathrm{SS}}_3}}\right) \\ K_{14} = \frac{1}{2}\cdot\frac{c_{\mathrm{HV-103}}}{A_{\mathrm{TK-100}}}\cdot\sqrt{\frac{G_{\mathrm{f}}}{P^{\mathrm{SS}}_1+\rho\cdot g\cdot H^{\mathrm{SS}}-P^{\mathrm{SS}}_3}} \end{cases} \tag{13}$$

$$\begin{cases} K_{21} = -\frac{U\cdot A_{\mathrm{h}}}{V_{\mathrm{TK-100}}\cdot c_{\mathrm{v}}\cdot\rho} \\ K_{22} = \frac{c_{\mathrm{p}}\cdot c_{\mathrm{LV-102}}\cdot T^{\mathrm{SS}}_1}{V_{\mathrm{TK-100}}\cdot c_{\mathrm{v}}}\cdot\sqrt{\frac{P^{\mathrm{SS}}_1-P^{\mathrm{SS}}_2-\rho\cdot g\cdot(H^{\mathrm{SS}}-H_{\mathrm{d}})}{G_{\mathrm{f}}}} \\ K_{23} = \frac{c_{\mathrm{p}}\cdot c_{\mathrm{LV-102}}\cdot VP^{\mathrm{SS}}_{\mathrm{LV-102}}}{V_{\mathrm{TK-100}}\cdot c_{\mathrm{v}}}\cdot\sqrt{\frac{P^{\mathrm{SS}}_1-P^{\mathrm{SS}}_2-\rho\cdot g\cdot(H^{\mathrm{SS}}-H_{\mathrm{d}})}{G_{\mathrm{f}}}} \\ K_{24} = \frac{1}{2}\cdot\left(\frac{c_{\mathrm{p}}\cdot c_{\mathrm{LV-102}}\cdot T^{\mathrm{SS}}_1\cdot VP^{\mathrm{SS}}_{\mathrm{LV-102}}}{V_{\mathrm{TK-100}}\cdot c_{\mathrm{v}}}\cdot\sqrt{\frac{G_{\mathrm{f}}}{P^{\mathrm{SS}}_1-P^{\mathrm{SS}}_2-\rho\cdot g\cdot(H^{\mathrm{SS}}-H_{\mathrm{d}})}}-\right. \\ \left.-\frac{c_{\mathrm{p}}\cdot c_{\mathrm{HV-103}}\cdot T^{\mathrm{SS}}_3}{V_{\mathrm{TK-100}}\cdot c_{\mathrm{v}}}\cdot\sqrt{\frac{G_{\mathrm{f}}}{P^{\mathrm{SS}}_1+\rho\cdot g\cdot H^{\mathrm{SS}}-P^{\mathrm{SS}}_3}}\right) \\ K_{25} = \frac{1}{2}\cdot\frac{c_{\mathrm{p}}\cdot c_{\mathrm{HV-103}}\cdot T^{\mathrm{SS}}_3}{V_{\mathrm{TK-100}}\cdot c_{\mathrm{v}}}\cdot\sqrt{\frac{G_{\mathrm{f}}}{P^{\mathrm{SS}}_1+\rho\cdot g\cdot H^{\mathrm{SS}}-P^{\mathrm{SS}}_3}} \\ K_{26} = -\frac{1}{2}\cdot\frac{c_{\mathrm{p}}\cdot\rho\cdot g}{V_{\mathrm{TK-100}}\cdot c_{\mathrm{v}}}\cdot\left(c_{\mathrm{LV-102}}\cdot T^{\mathrm{SS}}_1\cdot VP^{\mathrm{SS}}_{\mathrm{LV-102}}\cdot\sqrt{\frac{G_{\mathrm{f}}}{P^{\mathrm{SS}}_1-P^{\mathrm{SS}}_2-\rho\cdot g\cdot(H^{\mathrm{SS}}-H_{\mathrm{d}})}}-\right. \\ \left.-c_{\mathrm{HV-103}}\cdot T^{\mathrm{SS}}_3\cdot\sqrt{\frac{G_{\mathrm{f}}}{P^{\mathrm{SS}}_1+\rho\cdot g\cdot H^{\mathrm{SS}}-P^{\mathrm{SS}}_3}}\right) \end{cases} \tag{14}$$

$$\begin{cases} K_{31} = -\frac{U\cdot A_{\mathrm{h}}}{C_{\mathrm{M}}} \\ K_{32} = \frac{c_{\mathrm{TV-101}}\cdot\lambda_{\mathrm{s}}}{C_{\mathrm{M}}}. \end{cases} \tag{15}$$

$$\begin{cases} \dot{\hat{\mathbf{x}}} = \mathbf{A_m}\cdot\hat{\mathbf{x}} + \mathbf{B_m}\cdot\hat{\mathbf{u}} \\ \hat{\mathbf{y}} = \mathbf{C_m}\cdot\hat{\mathbf{x}} + \mathbf{D_m}\cdot\hat{\mathbf{u}}. \end{cases} \tag{16}$$

$$\begin{cases} \hat{\mathbf{x}} = \hat{\mathbf{y}} = \left[\hat{h}(t), \hat{T}_3(t), \hat{T}_{\mathrm{s}}(t)\right]^{\mathrm{T}}, \\ \hat{\mathbf{u}} = \left[\widehat{vp}_{\mathrm{LV-102}}(t), \widehat{vp}_{\mathrm{TV-101}}(t), \hat{P}_1(t), \hat{P}_3(t), \hat{T}_1(t)\right]^{\mathrm{T}} \end{cases} \tag{17}$$

$$\mathbf{A_m} = \begin{bmatrix} K_{11} & 0 & 0 \\ K_{26} & K_{21} & K_{21} \\ 0 & -K_{31} & K_{31} \end{bmatrix}, \mathbf{B_m} = \begin{bmatrix} K_{12} & 0 & K_{13} & K_{12} & 0 \\ K_{22} & 0 & K_{24} & K_{25} & K_{23} \\ 0 & K_{32} & 0 & 0 & 0 \end{bmatrix},$$
$$\mathbf{C_m} = \begin{bmatrix} 1 & 0 & 0 \\ 0 & 1 & 0 \\ 0 & 0 & 1 \end{bmatrix}, \mathbf{D_m} = \begin{bmatrix} 0 & 0 & 0 & 0 & 0 \\ 0 & 0 & 0 & 0 & 0 \\ 0 & 0 & 0 & 0 & 0 \end{bmatrix}, \tag{18}$$

4(a) and (b) respectively. From Fig. 3(a) and 4(a) it can be seen that both $\hat{h}(t)$ and $\hat{T}_3(t)$ reach a steady state value, where the slowest dynamics is that corresponding to $\hat{T}_3(t)$. On the other hand, and according to Fig. 3(b) and Fig. 4(b) it can be concluded that the transfer functions shown in (20) and (21) are stable, since all the poles are located on the left side of the s-plane.

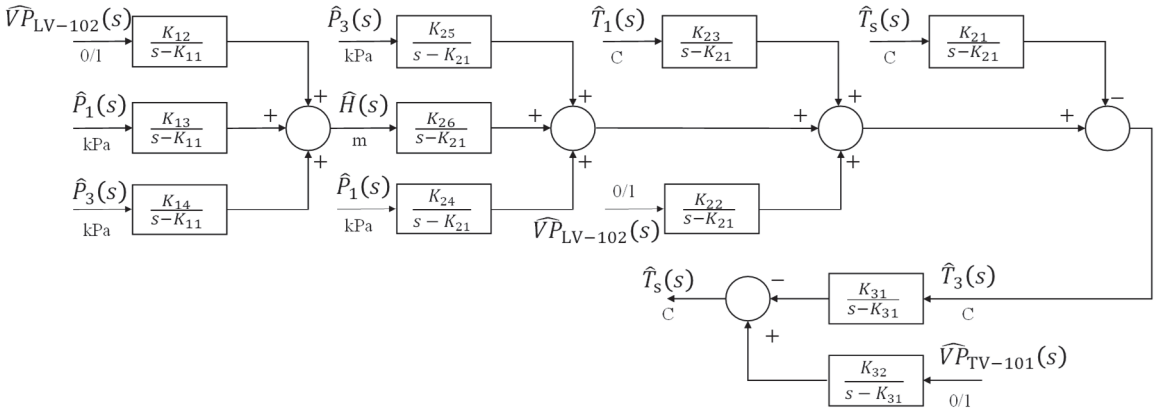

Fig. 2. Open-loop block diagram of the linearized model shown in (19).

$$\begin{cases} \hat{H}(s) = \frac{K_{12}}{s-K_{11}} \cdot \widehat{VP}_{LV-102}(s) + \frac{K_{13}}{s-K_{11}} \cdot \hat{P}_1(s) + \frac{K_{14}}{s-K_{11}} \cdot \hat{P}_3(s) \\ \hat{T}_3(s) = -\frac{K_{21}}{s-K_{21}} \cdot \hat{T}_s(s) + \frac{K_{22}}{s-K_{21}} \cdot \widehat{VP}_{LV-102}(s) + \frac{K_{23}}{s-K_{21}} \cdot \hat{T}_1(s) + \frac{K_{24}}{s-K_{21}} \cdot \hat{P}_1(s) + \frac{K_{25}}{s-K_{21}} \cdot \hat{P}_3(s) + \frac{K_{26}}{s-K_{21}} \cdot \hat{H}(s) \\ \hat{T}_s(t) = -\frac{K_{31}}{s-K_{31}} \cdot \hat{T}_3(s) + \frac{K_{32}}{s-K_{31}} \cdot \widehat{VP}_{TV-101}(s), \end{cases} \quad (19)$$

TABLE II. PARAMETERS OF TRANSMITTERS TT-101 AND LT-102

Parameters	Values
K_{TT-101}	1 TO%/°C
K_{LT-102}	109.769 TO%/m
τ_{TT-101}	0.05 s
τ_{LT-102}	0.01 s

TABLE III. TUNING PARAMETERS OF COMPENSATOR $G_{c1}(s)$ AND $G_{c2}(s)$.

Tuning parameters	Values
k_{pc1}	0.006
k_{ic1}	$9.152 \cdot 10^{-5}$
k_{pc2}	0.096
k_{ic2}	$3.96 \cdot 10^{-4}$

Using this information provided by Fig. 3 and 4 and with the aid of MATLAB-Simulink (with the SISOTOOL command), the PI compensators related to the TIC-101 and LIC-102 control loops are designed. It should be noted that SISOTOOL is based on the root locus analysis method [12]–[14].

Fig. 5 shows the block diagram of the closed-loop process, including the PI compensators and the TT-101 and LT-102 transmitters (red-dash lines). Fig. 5 shows the saturators connected to the output of the PI compensators, in order to prevent the control valves, i.e., TV-101 and LV-102, to receive non-binary signals. Finally, the transfer function of the compensators is shown in (22). Here k_p and k_i are the proportional and integral gains of the G_c respectively.

$$G_c(s) = k_p \frac{\left(s + \frac{k_i}{k_p}\right)}{s}. \quad (22)$$

The design of the PI compensators related to the LIC-102 and TIC-101 controllers, i.e., $G_{c1}(s)$ and $G_{c2}(s)$ respectively, provides the tuning parameters of each of the compensators listed in Table III. Fig. 6(a) and (b) show the responses to a step change associated with the TIC101 and LIC-102 controllers, respectively, which are described by the red dash lines in Fig. 5. From Fig. 6, it can be observed that both measured variables, i.e., $\hat{T}_3(t)$ and $\hat{h}(t)$ reach a steady state value, showing that the dynamics of LIC-102 and TIC-101 are stable.

B. LQR Design

Regarding the design of the LQR, which is based on optimal control techniques [9], [10], the state equation of (16) is considered, i.e., $\dot{\hat{\mathbf{x}}} = \mathbf{A_m} \cdot \hat{\mathbf{x}} + \mathbf{B_m} \cdot \hat{\mathbf{u}}$. On the other hand, the optimal control law $\hat{\mathbf{u}} = -\mathbf{K} \cdot \hat{\mathbf{x}}$ is defined in order to minimize the cost function shown in (23).

$$J = \int_0^\infty (\hat{\mathbf{x}}^T \cdot \mathbf{Q} \cdot \hat{\mathbf{x}} + \hat{\mathbf{u}}^T \cdot \mathbf{R} \cdot \hat{\mathbf{u}}) \cdot dt, \quad (23)$$

where $\mathbf{Q}$ and $\mathbf{R}$ are positive definite Hermitian matrices [9], [10]. Matrix $\mathbf{K}$ is a matrix with optimal values that is determined from the solution of the Riccati equation [9], [10], [12] and matrices $\mathbf{Q}$ and $\mathbf{R}$ are defined in (24).

As the LQR algorithm is conceptualized as a regulator and thus operates with zero references [9], [10]. it is necessary to customize the algorithm to apply it to the oil-heating tank, since, in this case, there are references different from zero, obviously.

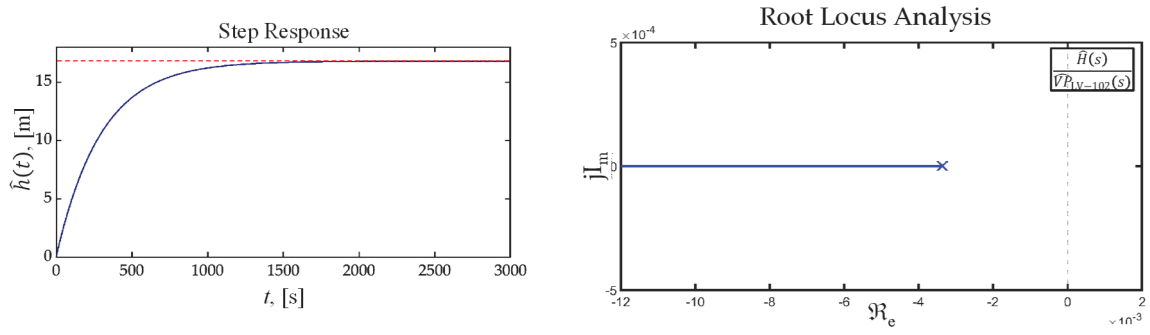

(a) (b)

Fig. 3. Transient analysis and root locus diagram regarding (20). (a) Step response. (b) Root-locus diagram..

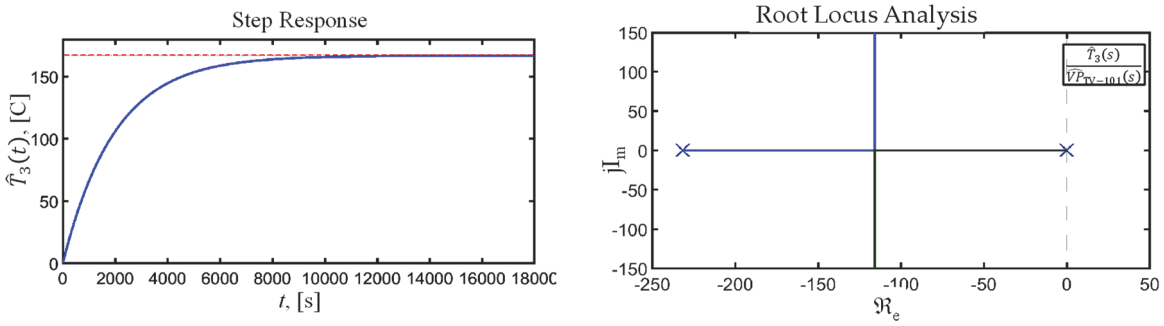

(a) (b)

Fig. 4. Transient analysis and root locus diagram regarding (21). (a) Step response. (b) Root locus diagram.

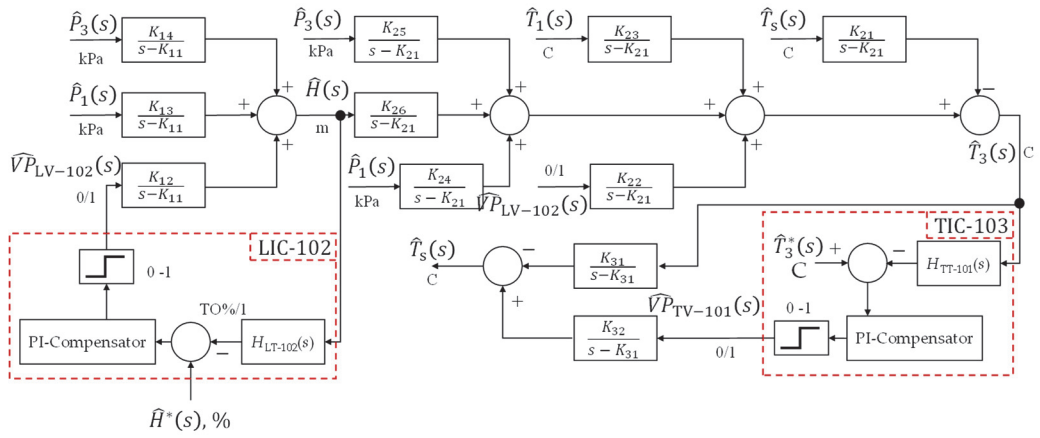

Fig. 5. Closed-loop block diagram of the oil-heating tank model, including PI compensators and measurement transmitters.

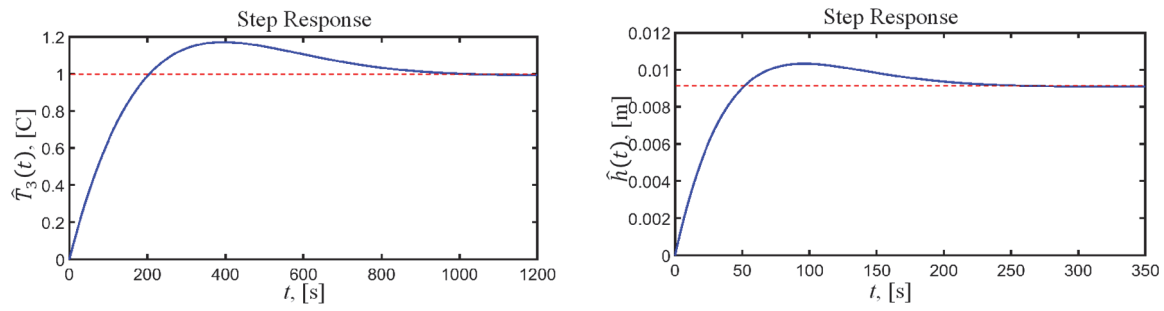

(a) (b)

Fig. 6. Step response of closed-loop transfer functions LIC-102 and TIC-101. (a) TIC-101. (b) LIC-102.

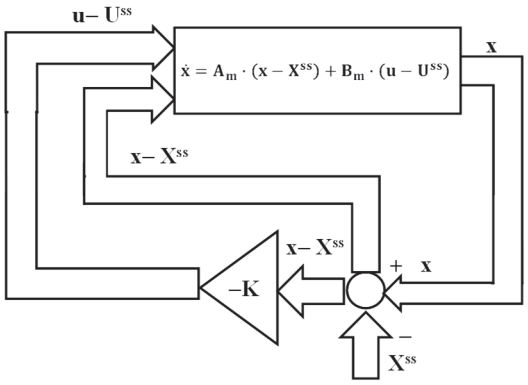

Fig. 7. Block diagram of LQR configured with non-zero references.

$$\mathbf{Q} = \begin{bmatrix} 100 & 0 & 0 \\ 10 & 0 & 0 \\ 0 & 0 & 0.01 \end{bmatrix},$$

$$\mathbf{R} = \begin{bmatrix} 1 & 0 & 0 & 0 & 0 \\ 0 & 1 & 0 & 0 & 0 \\ 0 & 0 & 1 & 0 & 0 \\ 0 & 0 & 0 & 1 & 0 \\ 0 & 0 & 0 & 0 & 1 \end{bmatrix}. \quad (24)$$

First, the steady-state vector is defined, which operates as a vector that takes into account the reference values, i.e. $\mathbf{X^{ss}} = [H^{ss}, T_3{}^{ss}, T_s{}^{ss}]^T$, $\mathbf{X^{ss}} \in \{\mathbb{R}^3\}$. A vector is also defined based on the steady state inputs, i.e. $\mathbf{U^{ss}} = [VP_{\text{LV-102}}{}^{ss}, VP_{\text{TV-101}}{}^{ss}, P_1{}^{ss}, P_3{}^{ss}, T_1{}^{ss}]^T$, $\mathbf{U^{ss}} \in \{\mathbb{R}^5\}$. Then, redefining the dynamic equation in (16) and the control law, in terms of the absolute and steady state variables (see subsection 3), the optimized model involving the vectors $\mathbf{X^{ss}}$ and $\mathbf{U^{ss}}$ is obtained and shown in (25). In this case $\mathbf{x} = [h(t), T_3(t), T_s(t)]^T$, $\mathbf{x} \in \{\mathbb{R}^3\}$, $\mathbf{u} = [vp_{\text{LV-102}}(t), vp_{\text{TV-101}}(t), P_1(t), P_3(t), T_s(t)]^T$, $\mathbf{u} \in \{\mathbb{R}^5\}$.

By using the MATLAB command *lqr*, the optimal matrix **K** is obtained and shown in equation (26). The eigenvalues of the optimized model (25) are presented in vector **E** (26), which correspond to negative values, indicating that (25) is stable [9], [10]. Fig. 7 shows the LQR diagram incorporated in model (25).

$$\begin{cases} \dot{\mathbf{x}} = \mathbf{A_m} \cdot (\mathbf{x} - \mathbf{X^{ss}}) + \mathbf{B_m} \cdot (\mathbf{u} - \mathbf{U^{ss}}) \\ (\mathbf{u} - \mathbf{U^{ss}}) = -\mathbf{K} \cdot (\mathbf{x} - \mathbf{X^{ss}}) \end{cases} \quad (25)$$

$$\mathbf{K} = \begin{bmatrix} 4.8344 & 2.7554 & 0.0038 \\ -8.8926 & 1.5386 & 0.0035 \\ 0.0000 & 0.0000 & 0.0000 \\ -0.0002 & 0.0000 & 0.0000 \\ -0.0533 & 0.0092 & 0.0000 \end{bmatrix},$$

$$\mathbf{E} = \begin{bmatrix} -0.0924 \\ -1.6262 \\ -231.6433 \end{bmatrix}. \quad (26)$$

V. Simulation Results

Simulations of the lossless linear model represented by (16) were carried out in MATLAB-Simulink. The process parameters and variables are listed in Table I.

It is assumed that the oil-heating tank is operating at steady state conditions with a level of H^{ss} = 50 % with an oil temperature inside the TK-100, $T^{ss}{}_3$ = 93.33 °C, a saturated steam temperature, $T^{ss}{}_s$ = 175 °C and a pressure $P^{ss}{}_1$ = 31.026 kPa. Then at 800 s there is a step change in $h^*(t)$ reaching a new steady state value of 30 %. Then at 1,000 s, $P_1(t)$ under-goes a perturbation decreasing the inlet oil pressure to 26.3721 kPa, and finally at 1,200 s a step change in $T_3(t)$ is generated reaching a new steady state value of 70 °C.

Fig. 8 shows the dynamics of the variables $h(t)$, $T_3(t)$, $vp_{\text{TV-101}}(t)$, $vp_{\text{LV-102}}(t)$, and $P_1(t)$, when the controller corresponds to a PI compensator and a LQR. Fig. 8(a) shows a comparison of the dynamics of $h(t)$, when the controller is an LQR (the blue one) and when it is a PI compensator (the cyan one), in addition the dynamics of $h(t)$ before being measured by the LT-102 transmitter is displayed (the green one). The red one is the reference value. Fig. 8(b) shows the comparison of the dynamics of $T_3(t)$ in the same format as Fig. 8(a). Fig. 8(c) shows the comparison of $P_1(t)$ dynamics and finally Fig. 8(d) and (e) are the comparisons of the dynamics of $vp_{\text{LV-102}}(t)$ and $vp_{\text{TV-101}}(t)$ valve positions respectively. It can be seen from Fig. 8(a) and (b) that the shortest settling times are presented by the dynamics $h(t)$ and $T_3(t)$ when the controller is an LQR instead of a PI compensator. In addition, from these same figures it is clear to see the effect that the time constants of the transmitters have on the display of the dynamics. The green dynamics shows the initial state of the level H^{ss} (50 %) and temperature $T_3{}^{ss}$ (93.33 °C), instead of the cyan figure, which is the dynamics of the level and temperature, coming from the transmitter LT-102 and TT-101 respectively, which, due to the effect of the time constants, the initial state of $h(t)$ and $T_3(t)$ are shown as 0 %.

On the other hand, from Fig. 8(a) and (b) it can be seen that when TIC-101 and LIC-102 controllers are PI compensators the step change in $h^*(t)$ and $T_3{}^*(t)$ generates disturbances in less magnitude than when the controllers are combined in a LQR in the variables $T_3(t)$ and $h(t)$ respectively. However, as mentioned above, the settling time is much longer when PI compensators are involved. Moreover, Fig. 8(c) also shows that the temperature dynamics $T_s(t)$, which is measured at the heating-coil output (see Fig. 1), has more stable dynamics when an LQR is applied instead of PI compensators. This feature is of key importance, since it is essential in this type of process to keep the temperature of the saturated

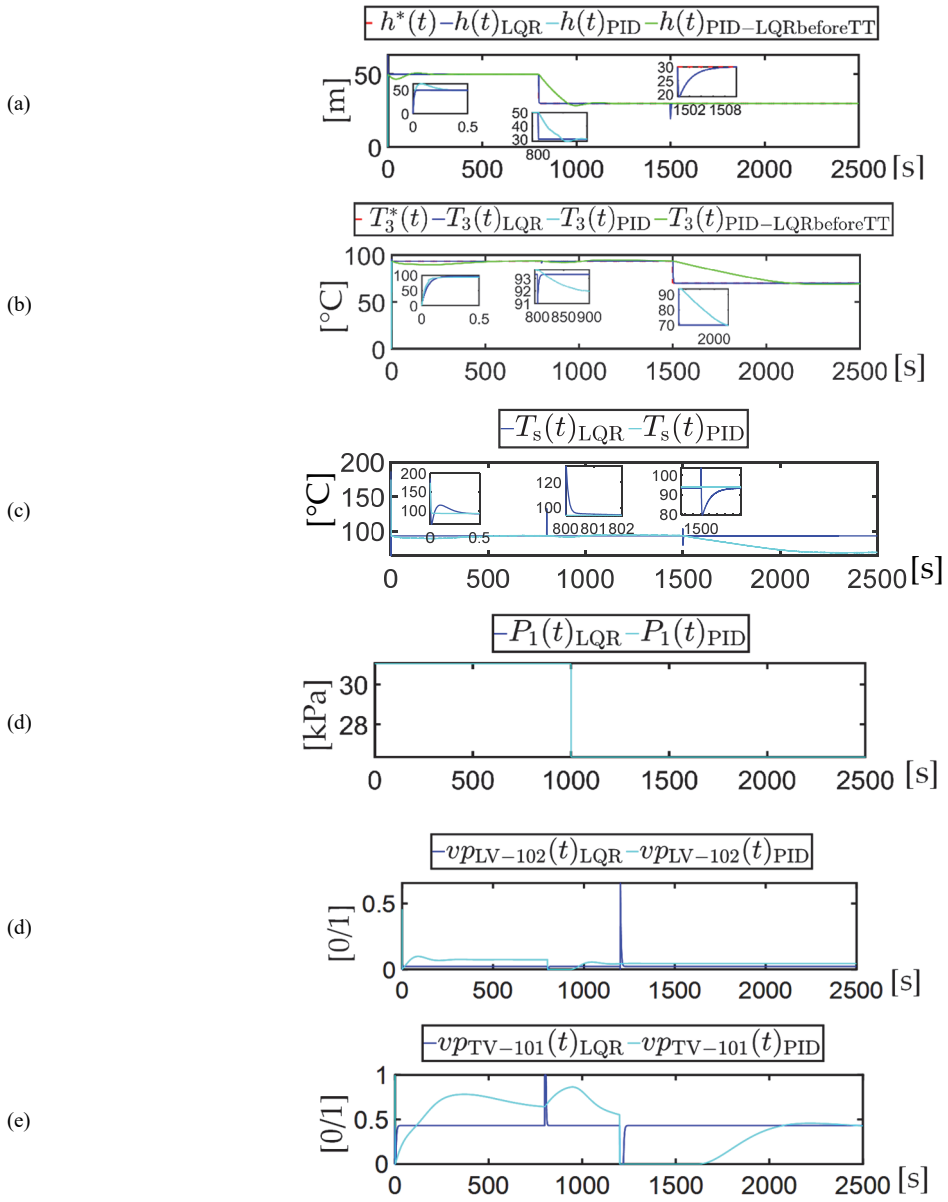

Fig. 8. Simulation results under transient operation. Reference level $h^*(t)$ = 50 %, temperature $T^*_3(t)$ = 93.33 C, and steady-state value of $P_1(t)$ = 31.026 kPa. A step change in $h^*(t)$ at 800 s, a step-change in $T^*_3(t)$ at 1,200 s, and a step-change in $P_1(t)$ at 1,000 s. (a) Level dynamics $h(t)$. (b) Temperature dynamics $T_3(t)$. (c) Temperature dynamics $T_s(t)$. (d) Pressure dynamics $P_1(t)$. (e) Valve position dynamics $vp_{\mathrm{LV-102}}(t)$. (f) Valve position dynamics $vp_{\mathrm{TV-101}}(t)$. All dynamics are overlapped and match when the controller is a LQR and when it is a PI compensator.

steam as stable as possible in order to reduce the cost of saturated steam production. It is well known that the generation of saturated steam is one of the main expenses in thermal or petro-chemical plants, where there are a large number of oil-heating tanks. It is interesting to note that, when an external disturbance occurs in $P_1(t)$ (see Fig. 8(d)), none of the variables presented in Fig. 8 is affected, showing then that the process with both types of controllers (PI and LQR) presents an important robustness. Finally, from Fig. 8(e) and (f) it can be seen that the behaviors of the valve positions $vp_{\mathrm{TV-101}}(t)$ and $vp_{\mathrm{LV-102}}(t)$ present a smoother modulation when the controllers are PI than when it is a LQR, However, when the controller is an LQR, $vp_{\mathrm{TV-101}}(t)$ and $vp_{\mathrm{LV-102}}(t)$ are more stable but involve some peaks, resulting in openings and closings at 100 % and 0 % respectively in a very short time, which could be harmful to the mechanical elements of these valves.

VI. Conclusion

The study of an oil-heating tank incorporating mathematical modeling and the de-sign of two linear controllers has been presented in this work. Based on the law of conservation of mass and energy applied to this process, the nonlinear dynamic equations that model the oil-heating tank are obtained. Then, the operating points of the steady-state process are calculated to finally linearize the

system using the Taylor expansion around the calculated operating points. As a result of the linearization, a state-space model of the oil-heating tank is obtained.

Using the state-space model, two proportional-integral compensators are designed; one to control the level of the oil-heating tank $h(t)$ and the other to regulate the outlet temperature of the processed oil $T_3(t)$. On the other hand, to regulate these same variables, a linear quadratic regulator is designed and the results of these controllers are compared.

In overall, and according to Fig. 8, it can be seen that the process with both types of linear controllers, i.e., the proportional-integral compensators and the linear quadratic regulator works properly, but in particular it can be concluded that the dynamics of the controlled variables, i.e., $h(t)$ and $T_3(t)$ when the process operates with two proportion-al-integral compensators working as controllers, present a longer settling time compared to the case when the process operates with a linear quadratic regulator. In addition, the dynamics of $h(t)$ and $T_3(t)$ show a better smoothness against produced disturbances.

On the other hand, when the process operates with a linear quadratic controller, the dynamics of $T_s(t)$ is much smoother than when operating with proportional-integral compensators, being a key factor the stability of this temperature, since the cost of the production of saturated steam has as a function, precisely the stability of its temperature.

Finally, it can be concluded that when the process is controlled with the proportion-al-integral compensators, the dynamics presented by the valve positions $vp_{\text{TV-101}}(t)$ and $vp_{\text{LV-102}}(t)$ present a smoother modulation although more variable than those shown when the controller is a linear quadratic regulator, However, when the process is controlled by the latter, the valve positions show certain peaks of 100% opening and absolute closures in very short periods of time, which can cause important damages to the mechanical elements of the valves.

REFERENCES

[1] T. Tomisa, S. Tešnjak, and I. Kuzle, 'Measurements and Modelling of Crude Oil Heating Process', May 2001.

[2] M. Semerak, S. Pozdeev, R. Yakovchuk, O. Nekora, and O. Sviatkevych, 'Mathematical modeling of thermal fire effect on tanks with oil products', *MATEC Web Conf.*, vol. 247, p. 00040, 2018, doi: 10.1051/matecconf/201824700040.

[3] H. Zhuang, F. Bai, and J. Xue, 'Modeling, simulation, and control of an oil heater', *IEEE Control Systems Magazine*, vol. 7, no. 4, pp. 41–44, Aug. 1987, doi: 10.1109/MCS.1987.1105336.

[4] A. Fuchs, D. R. Lewin, and S. J. Wajc, 'Modelling, simulation and control of a crude oil preheating furnace', *Chemical Engineering Science*, vol. 48, no. 4, pp. 661–679, Feb. 1993, doi: 10.1016/0009-2509(93)80134-C.

[5] F. Zhou, 'Numerical Simulation of Large Crude Oil Storage Tank Fire under Various Wind Speeds', *Journal of Physics: Conference Series*, vol. 1300, p. 012003, Aug. 2019, doi: 10.1088/1742-6596/1300/1/012003.

[6] C. A. Smith and A. B. Corripio, *Principles and Practice of Automatic Process Control, 2nd Edition*, 2nd edition. New York: Wiley, 1997.

[7] D. E. S. T. F. E. D. A. M. F. J. D. III, *Process Dynamics and Control by Dale E. Seborg*. 1656.

[8] W. L. Luyben, *Process Modeling, Simulation and Control for Chemical Engineers*, Subsequent edition. New York: McGraw-Hill College, 1989.

[9] J. Saffiro, 'Compute and Simulate Linear Quadratic Regulator (LQR) in MATLAB for Nonzero Set Points | Fusion of Engineering, Control, Coding, Machine Learning, and Science'. https://aleksandarhaber.com/compute-and-simulate-linear-quadratic-regulator-lqr-in-matlab-for-set-point-tracking/ (accessed Jul. 28, 2022).

[10] P. Dorato, C. T. Abdallah, and V. Cerone, *Linear Quadratic Control: An Introduction*. Melbourne, FL: Krieger Pub Co, 2000.

[11] M. Aktaş, Doç. D. Yusuf Altun, and O. Erol, *LQR Control of Liquid Level and Temperature Control for Coupled-Tank System*. 2017, p. 79.

[12] O. Katsuhiko, *Modern Control Engineering*. Boston, 2009.

[13] B. C. Kuo, *Automatic control systems*, 6th edition. Englewood Cliffs, N.J: Prentice Hall, 1991.

[14] *The Control Handbook (three volume set)*. CRC Press, 2018. doi: 10.1201/9781315218694.